Biophysical Journal Volume 65 October 1993 1700–1713

Composite Cylinder Models of DNA: Application to the Electrostatics of the B-Z Transition

J-P. Demaret* and M. Guéron‡

*Laboratoire de Physique et Chimie Biomoléculaires, Institut Curie et Université Paris VI, Paris, and ‡Groupe de Biophysique, Ecole Polytechnique, Palaiseau, France

ABSTRACT We develop and test a Poisson-Boltzmann model of the electrostatics of the B-Z transition of DNA. Starting from the detailed geometries of the two forms, we compute at each radius the fractions of DNA matter, of volume forbidden (for nonpointlike ions), and of volume accessible to the center of ions. These radial distributions are incorporated in a composite cylinder model; availability to ions (porosity) and the dielectric constant at each radial distance are then obtained. The phosphate charge is distributed with cylindrical symmetry on two layers at the appropriate radial distances. The *porous sheath*, between the axis and the charge distribution, provides much more room for ions in B-DNA than in Z-DNA.

By using previously developed methods, the Poisson-Boltzmann problem of such cylinders is easily solved. The computational load is small, so that results can be obtained for a large set of salt concentrations and for a number of ionic radii. The variation of the electrostatic free energy difference with salt concentration compares favorably with the experimental value (it is half as large). There is also qualitative agreement with experiments on supercoiled DNA, including a maximum of the free energy difference at submolar salt concentrations.

The results for this *cylinder with porous sheath* are in line with those of the earlier simple planar model and of a plain *cylinder with sheath*, which is also presented here. They are thus insensitive to details of the model. They support the proposition that the main electrostatic feature of the B-Z transition is the better immersion of the B-DNA phosphates into the solution. They also give confidence in the validity of the Poisson-Boltzmann approach, despite the large salt concentrations involved. Prior studies using an approach based on the potential of mean force are discussed.

1. INTRODUCTION

1.1. The Poisson-Boltzmann theory of the simple cylinder

In the study of polyelectrolytes in solution, both the geometry and the electrostatics are subject to drastic simplifications. If the solution is described as made of ions in a continuous solvent and if one ignores the correlations between ions due to their finite size and to their electrostatic interactions, one obtains the Poisson-Boltzmann equation.

The polyelectrolyte solute may be represented as a solid cylinder with a uniform superficial charge density s (Fuoss et al., 1951). This defines the electric field at the surface. With the further condition that the potential is zero at infinity, the electrostatic problem is completely defined. It can be solved by numerical integration. In particular, one obtains the surface potential, from which the free energy is computed by a charging procedure (Fixman, 1982).

The theory of such a *simple cylinder* can be described with reference to two limiting cases for which an analytical expression and a simple description of the *surface potential* are known. One limit is that of the weakly charged cylinder and the corresponding linearized Poisson-Boltzmann (or Debye-Hückel) theory; the required nonlinear corrections for strongly charged cylinders have been tabulated (Stigter, 1975). The other limit is that of a plane (a cylinder with zero curvature) having the same superficial charge density as the cylinder; the correction to the surface potential for finite curvature is obtained approximately in a perturbation framework and expressed algebraically (Weisbuch and Guéron, 1981, 1983). Based on such procedures, we have also derived algebraic formulas that provide an excellent approximation to the *free energy* of cylinders, whether highly or weakly charged (Guéron and Demaret, 1992a).

In the case of a highly charged cylinder, one finds that one-half of the polyelectrolyte charge is neutralized by counter-ions within a layer, the thickness *Th* of which is largely independent of the salt concentration, being approximately equal to $a/(z\xi)$, where a is the cylinder radius, z is the counter-ion valency, and ξ is the linear charge parameter, that is, the number of electronic charges within the Bjerrum length l_B (0.72 nm; see below) along the cylinder axis (ξ = 4.2 for B-DNA). The counter-ion concentration in the immediate vicinity of the polyelectrolyte surface (C_{IV}) is also nearly independent of the salt concentration. It is about 4 mol/liter for DNA (Guéron and Weisbuch, 1980).

The use of the Poisson-Boltzmann theory may be criticized since, being a mean-field theory, it ignores the correlations between ions due to their finite size and their electrostatic interaction. However, this is known to be less significant for the properties of polyelectrolytes in solution

Received for publication 8 March 1993 and in final form 22 July 1993.

Address reprint requests to Prof. Maurice Guéron, Groupe de Biophysique, Ecole Polytechnique, 91128 Palaiseau, France.

Abbreviations used: FED, free energy difference; CS, composite cylinder with a core and a sheath; CPS, composite cylinder with a core and a porous sheath.

0006-3495/93/10/1700/14 $2.00

than for those of ionic solutions (Fixman, 1979). The model also ignores the detailed geometry of the polyelectrolyte, the chemistry of its charged groups, and the finite size of the water molecules. Within the Poisson-Boltzmann framework, these properties may be partially taken into account by modifications of parameters such as cylinder radius and linear charge density, and perhaps, in a more refined treatment, by the use of a distance-dependent dielectric constant for the solvent (Hingerty et al., 1985). As long as one does not search for detailed quantitative results, which in any case are often out of reach for reasons of complexity rather than principle, such refinements may not be required.

The Poisson-Boltzmann/simple cylinder model has been applied to many questions, including the influence of shape on the properties of highly charged polyelectrolytes and the concentration of counter-ions at the polyelectrolyte surface in solutions of monovalent ions or in solutions containing both monovalent and divalent cations (Guéron and Weisbuch, 1980). Local interactions with counter-ions may be modeled after those occurring between an isolated monomer constituent of the polyelectrolyte and counter-ions in a solution, the concentration of which is the surface concentration just mentioned. The model also provides for the interpretation of colligative properties (Guéron and Weisbuch, 1979).

The results are generally in fair agreement with experiment because the model accounts for the main feature of the system: *an enhanced counter-ionic concentration near the polyelectrolyte*. But one must be aware that the experiments generally involve features other than the strictly electrostatic ones and therefore do not provide a severe test of the model.

On the other hand, there is no reason to expect that the simple cylinder is adequate for studying the effects of *structural variations* of the polyelectrolyte, since it can describe them only through changes in radius and linear charge. The B-Z transition of DNA (Pohl and Jovin, 1972; Pohl, 1983) is an example of such a structural variation, which the simple cylinder model fails to describe (Soumpasis, 1984; Frank-Kamenetskii et al., 1985). But, as we shall see, the variations can be incorporated into a modified model, without abandoning either the cylindrical symmetry or the Poisson-Boltzmann theory.

1.2. The B-Z transition

The transition of double-stranded DNA ($d(CG)_n$ sequences) between right-handed B-DNA and left-handed Z-DNA (Wang et al., 1979) at high salt concentrations provides an interesting test for polyelectrolyte theories. From measurements on synthetic fragments of different lengths, one obtains the *free energy difference* (FED) between the B and Z forms as a function of the salt concentration (Pohl, 1983). If the effect of salt is mainly electrostatic in origin, so is the *variation in the FED*, and electrostatic theories may be checked against it. It is unfortunate that the range of salt concentrations accessible to such studies is limited (1–5 M) and that comparable explorations at different temperatures or with different salts have not been reported.

The B-Z equilibrium is sensitive to other parameters, such as temperature (Behe et al., 1985), pressure (Krzyzaniak et al., 1991), the composition of a water-alcohol solvent (Pohl, 1976), bromination of guanosine (Lafer et al., 1981), 5-methylation of cytidine (Behe and Felsenfeld, 1981), association with proteins (Lafer et al., 1986), or supercoiling by inclusion of the $d(CG)_n$ sequence in circular DNA (Stirdivant et al., 1982). The Z form is also reported in low concentrations of multivalent ions (Van de Sande et al., 1982) and of monovalent ions (Ivanov et al., 1987; Sági et al., 1991).

On the theoretical side, it has been proposed that the preference for the Z form in high salt is due to screening of the repulsion between phosphate charges, some of which are closer in the Z form than in the B form (Arnott et al., 1975; Wang et al., 1981). Quantitatively, the B-Z transition has been studied using the Poisson-Boltzmann/simple cylinder model (Frank-Kamenetskii et al., 1985). The variation with salt of the electrostatic free energy of the Z form with respect to the B form in high salt was dependent on the choice of the cylinder radii. At best, the computed increase in the stability of the Z form was 50 times smaller than what was observed. At very low ionic strength, the Z form was also favored.

Previously it had been proposed that the electrostatic and geometric imperfections of the Poisson-Boltzmann/simple cylinder model could be too severe for the treatment of the B-Z transition (Soumpasis, 1984). The DNA charge was therefore represented in more detail, as hard spheres located at each phosphate position. However, the rest of the molecule was omitted and replaced with solution. The free energy was computed using a potential of mean force theory to account for inter-ionic correlations. The variation of the electrostatic FED could be fitted to the high-salt experiment by an appropriate choice for the distance of closest approach between ions.

1.3. Scope of this work

The motivation for the present work was the belief that *more attention should be given to the major geometric features of the transition and that a simple electrostatic theory would suffice* (Guéron and Demaret, 1992b). Our approach to the geometric and electrostatic approximations is based on *three considerations:*

(*a*) Regarding the DNA geometry: one should treat with particular care the differences between B-DNA and Z-DNA. One difference that is conspicuous on the crystallographic structures is that the grooves are larger in B-DNA; there is more room for water and counter-ions. The phosphates, being located at the rim of the grooves, are further from the neutral DNA core. They are better immersed in the solution and therefore more susceptible to screening by counter-ions than in the Z form. Better screening should increase the

relative stability of the B form in medium salt (versus high salt), thus providing a qualitative explanation for the B-Z transition.

(*b*) In contrast to this effect of neutral DNA matter on the relative disposition of counter-ions and phosphates, the other geometric and electrostatic factors affecting *correlations between ions* (i.e., between a counter-ion and a phosphate, between two counter-ions, etc.) are similar for B-DNA and Z-DNA, and their effect on the free-energy difference should be smaller.

(*c*) The two features just described are not related to any *micro*molecular feature of DNA geometry. They can therefore be incorporated into a cylindrical model obtained by cylindrical averaging.

These considerations suggest that the Poisson-Boltzmann theory of an appropriate cylindrical model should be able to describe the B-Z transition. This was indeed shown recently for a crude but easily computed model, one where B-DNA and Z-DNA were replaced by charged planes with two or one sides, respectively, in the solution (Guéron and Demaret, 1992b). In the present paper, we develop cylindrical models that are appropriate for the study of the B-Z transition. Our goal is not to improve on the result of the planar model. Rather, we want to demonstrate that success persists in a more refined—if more complex—model of DNA geometries: the "composite cylinder." A second goal of the study of the composite cylinder is the investigation of the relative stability of B- and Z-DNA in low salt (<1 mM), for which the planar model is inadequate. Last, the successful treatment of the B-Z transition suggests that the composite cylinder model provides a good electrostatic description of DNA and may therefore be useful for other problems.

In section 2 we examine the geometries of B- and Z-DNA. We determine the radial distributions of DNA matter and of solution, distinguishing between the volume accessible to the center of an ion and that inaccessible to it. As expected, the accessible volume between the DNA axis and the phosphate charges is distinctly larger for B- than for Z-DNA. The numerical measurements are carried out for four values of the counter-ion radius. The results are used for the development of two composite cylinder models of DNA.

The first model, the *composite cylinder with a core and a sheath* (CS), has an impenetrable core, surrounded by a sheath of solution within a charged cylindrical surface. The second model, the *composite cylinder with a core and a porous sheath* (CPS), provides a more detailed representation of the radial distributions of DNA charge, of DNA neutral matter, and of the volume inaccessible to counter-ions.

In section 3, we develop the electrostatic theory of the CS and CPS models and compute the potential at the charged surfaces. The computation also provides the ionic content within the sheath and hence the net charge of the composite cylinder. In section 4 we compute the free energy of the models, apply the results to the B-Z transition, and compare them to the experimental data. In section 5 the usefulness of the Poisson-Boltzmann theory and of composite cylinder models is discussed on the basis of the present results and of those obtained with other models.

2. CYLINDRICAL AVERAGING OF THE B-DNA AND Z-DNA GEOMETRIES

2.1. DNA geometry

We first consider the location of DNA charges. The charge of a phosphate group is mostly located on the two singly liganded oxygens. The radial distances of their centers, which we shall consider to be the location of a charge $e/2$, are given in Table 1, derived from the crystallographic data (Arnott et al., 1975; Wang et al., 1981). The latter correspond to Z-DNA type I; type II is not considered here. In B-DNA, there are two different radial distances. In Z-DNA, there are four, because the guanosine and cytidine phosphate are not placed equivalently.

In order to evaluate the space available to counter-ions, we have determined the surface that limits the volume that is inaccessible to the center of a counter-ion, using the Molecular Surface program of M. L. Connolly (1983). This program rolls a sphere of given radius in contact with the atomic DNA surface and records the surface generated by the center of the sphere, as sketched in Fig. 1. In the case of a nearly pointlike ion (r = 0.02 nm), the surface is close to that of DNA itself. When the ion is larger (the radius is 0.095 nm for sodium, 0.4 nm for hydrated sodium), parts of the inaccessible volume are occupied by water. The computations were carried out on a model spanning two base pairs, but all the geometric results (volumes, height h along the cylinder axis) are expressed per base pair.

Fig. 2 displays the volumes accessible and inaccessible to the center of an ion within a given distance of the DNA axis. The volumes are represented in a derivative mode.

For example, the volume of DNA within the radius R corresponding to the label A (Fig. 2 *a*) is proportional to the area limited by the horizontal axis up to A, the vertical line AB, and the full curve connecting the origin O to B. The total volume ($\pi R^2 h$) is represented by the area of the triangle OAE, and the volume of solution corresponds to the area limited by the full curve OB and the straight lines BE and EO. The volume of solution is also the volume accessible to pointlike ions. The volume accessible to the center of ions with a finite radius is smaller; for ions of radius 0.235 nm it is represented by the small area between OE, OD, and DE, and there is no volume accessible at all to an ion of radius 0.4 nm.

The radial positions of the charged oxygens (r_1 to r_4 in Table 1) are marked by arrows. A radius of charge b is defined as the average of the four radii. A comparison of the two panels in Fig. 2 shows that the volume $V(b)$ available to the centers of ions within the radius of charge b is larger in B-DNA than in Z-DNA, mainly because b is larger in the former (0.961 nm) than in the latter (0.667 nm). For an ionic radius of 0.4 nm the volumes $V(b)$ are 0.168 and 0.043 nm^3 per base pair in B- and Z-DNA, respectively (Table 1). We note that with an ionic concentration of 3.3 mol/liter, which is in the range of the surface concentration for DNA, a vol-

TABLE 1 Geometric parameters of B-DNA* and Z-DNA‡

	B-DNA				Z-DNA			
r_1§	0.892				0.649			
r_2	1.029				0.669			
r_3	0.892				0.684			
r_4	1.029				0.860			
b¶	0.961				0.716			
b'‖					0.667			
Axial height h	0.338				0.372			
Ion radius**	0.02	0.095	0.235	0.4	0.02	0.095	0.235	0.4
X‡‡	0.505	0.608	0.836	1.204	0.505	0.645	0.923	1.371
$V(b)$§§	0.511	0.461	0.335	0.158	0.212	0.157	0.105	0.025
$X(b)$	0.469	0.519	0.645	0.822	0.386	0.441	0.493	0.573
$X_{out}(b)$	0.036	0.089	0.191	0.382	0.119	0.204	0.430	0.798
$V(b')$					0.172	0.131	0.089	0.016
$X(b')$					0.348	0.389	0.431	0.504
$X_{out}(b')$					0.157	0.256	0.492	0.867
$V(r_4)$					0.386	0.302	0.166	0.069
$X(r_4)$					0.478	0.562	0.698	0.795
$X_{out}(r_4)$					0.027	0.083	0.225	0.576

*Derived from Arnott et al. (1975).
‡Derived from Wang et al. (1979).
§Radial distance of charged phosphate oxygens. All distances are in nm.
¶Average of r_1, r_2, r_3, r_4.
‖Average of r_1, r_2, r_3.
**The four columns correspond successively to ionic radii of 0.02 ("pointlike" ion), 0.095 (sodium), 0.235, and 0.4 nm (hydrated sodium).
‡‡X is the total volume forbidden to the centers of ions. For ions of 0.02 nm radius, this is close to the volume of DNA. Volumes are in nm^3, for an axial height of one base pair.
§§Volume accessible (V) and not accessible (X) to centers of ions within radii b, b', and r_4. $X_{out}(x)$ is the nonaccessible volume beyond radius x.

ume of 0.5 nm^3 contains one ion, equivalent to one-half of the phosphate charge of a base pair. Thus, the effect of the ions within $V(b)$ on the net charge of DNA should be significant and much larger for B- than for Z-DNA.

As the ionic radius grows, $V(b)$ becomes smaller. The center of a bulky ion (e.g., r = 0.8 nm) would be kept further from the axis than the phosphate charges, and simple cylinder models would become appropriate.

2.2. Cylindrical models

In Fig. 2, we have a cylindrical average of the distribution of matter in the atomic DNA geometry. We now describe two cylindrical models that will be the subject of the Poisson-Boltzmann analysis.

2.2.1. A cylinder with core and sheath: the CS model

In this model, the charges are represented by a uniform distribution on a single cylinder placed at their average distance, b, from the axis. A sheath of solution, accessible to the centers of ions, is located between an impenetrable cylindrical core (radius c) and the b cylinder (Fig. 3). Beyond b, any volume $X_{out}(b)$ inaccessible to centers of ions (including DNA matter) is ignored and replaced by solution. The core radius is chosen so that the volume of the sheath is equal to the volume accessible to ion centers within b (i.e., $V(b)$ as defined in section 2.1). The core radius c is therefore derived by $\pi h(b^2 - c^2) = V(b)$. With this definition, the core volume (πhc^2) is equal, as it should be, to the volume that is inaccessible to ion centers (the DNA volume, in the case of pointlike ions) within radius b. The geometry is illustrated in Fig. 3.

The CS model is intermediate between the planar model analyzed previously (Guéron and Demaret, 1992b) and the model with porous sheath described below.

2.2.2. A cylinder with core and porous sheath: the CPS model

This model provides a more detailed description of the distributions of charge and of matter. The *charge* is distributed on two cylinders. For B-DNA their radii correspond to the locations of oxygen, r_1 and r_2, and each bears half of the charge. For Z-DNA, three-fourths of the charge is on a cylinder, the radius of which (b') is the average of the radii r_1, r_2, r_3, which are close together (Table 1). One-fourth of the charge is on a cylinder of radius r_4. The distribution of DNA *matter* is the true cylindrical average depicted in Fig. 2.

The porous medium. In the simple cylinder model, DNA matter defines the cylinder radius a, within which there is no solution and hence no ions, and beyond which there is no DNA matter. Hence the potential distribution beyond a is unaffected either by the radial position of the DNA charges, or by the properties (dielectric constant, etc.) of the DNA matter. Ions of finite size alter this picture only by a dilation of the cylinder.

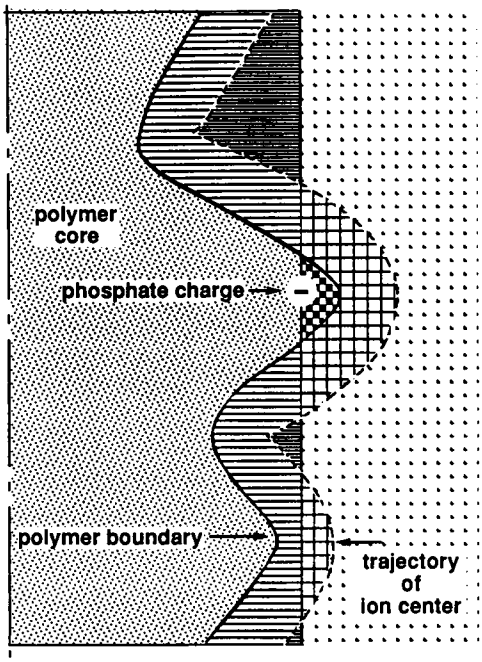

FIGURE 1 Representation of the internal and external volumes for a fragment of an imaginary DNA-like polyelectrolyte. The helical axis and the location of charges are indicated. The grooves give rise to a volume V_{sh} accessible to ions, in the region closer to the axis than the polyelectrolyte charges. Polyelectrolyte matter beyond the radius of the charges generates a volume X_{out} inaccessible to the center of ions. For a nearly pointlike ion, V_{sh} includes the regions filled by tight and by loose horizontal lines; X_{out} is marked by checkerboards. For an ion of finite radius, V_{sh} is smaller (tight horizontal lines) and X_{out} is larger (checkerboards and squares).

In a more detailed model, however, the distribution of DNA matter is important. On one hand, there is room for counter-ions to be closer to the axis than are the charged cylinders, the potential of which is thus reduced. On the other hand, some regions between the charged cylinders, or beyond, may be occupied by DNA matter, so that they are inaccessible to counter-ions. This will also affect the potential. In the CPS model, one finds at each radius three components, in the proportions of the true cylindrical average (Fig. 2). They are:

- DNA matter, for a fraction $f_{DNA}(r)$;
- space that belongs to the solution but is forbidden to ion centers, for a fraction $f_{forb}(r)$; this fraction is zero in the case of pointlike ions;
- and solution space accessible to ion centers, for a fraction $(1 - f_{DNA}(r) - f_{forb}(r))$.

The respective fractions can be read off Fig. 2. For instance, in the case of B-DNA at radius R, $f_{DNA}(R)$ is equal to AB/AE; $f_{forb}(R)$ is BC/AE for the naked sodium ion and BD/AE for an ionic radius of 0.235 nm. The DNA radius, a, defined as the radius beyond which only solution remains, depends on the ionic radius (Fig. 2 and Table 1).

The mixture of three components constitutes a medium the composition of which is a function of the radius. The medium is locally homogeneous. It is porous, in the sense that it can be penetrated by water and ions. The ionic concentration at radius r is $[1 - f_{DNA}(r) - f_{forb}(r)]$ times that of the solution, since the quantity in brackets is the fraction of the volume accessible to ions.

Dielectric constant in the porous medium. Of the three components of the porous medium (solution, volume forbidden due to finite ion size, and DNA matter), the first two have the dielectric constant of water (D_w). In regions where ions are present, the third component, DNA matter, comes mostly from the hydrophilic backbone, the dielectric constant of which is certainly larger than the value of 2 commonly used as an average for DNA matter. The value chosen for D_{DNA} affects only weakly the average dielectric constant. We choose $D_{DNA} = 5$ arbitrarily.

The dielectric constant $D(r)$ is the weighted average of the dielectric constants of the three components

$$D(r) = D_{DNA} f_{DNA}(r) + D_w(1 - f_{DNA}(r)) \quad (1)$$

2.3. Ion radius

The radius of a bare sodium ion is 0.095 nm, that of hydrated sodium is 0.4 nm if electrostriction is ignored, and that of nonhydrated chlorine is 0.181 nm. It is customary to consider alkali cations to be hydrated and larger anions not to be. Indeed, in the definition of the DNA surface, we assumed that the phosphodiester anions, like the sugars and bases, were not hydrated.

As for the cations, their full hydration is far from certain. In crystals of ApU, sodium ions are directly coordinated, one to a uracil carbonyl, one to a phosphodiester oxygen (Rosenberg et al., 1973). Dehydration of alkali cations (in contrast to larger organic cations) in the vicinity of polyelectrolyte is also indicated by the measurement of ion volume (Tondre and Zana, 1972, 1975) and by theoretical studies (Prasad and Pack, 1984; Pack et al., 1991). We choose 0.235 nm for the Na^+ radius, a value intermediate between those noted above. We shall see that this choice has only a moderate effect on the theoretical results, which can be tested presently.

The DNA model used here assumes a single value of the radius for counter-ions and co-ions alike. An error in co-ion radius, resulting from this contraint, is of little consequence in low salt since the surface potential is large, so that the local concentration of co-ions is small. But in high salt the error in local co-ion concentration could be significant.

3. ELECTROSTATICS OF THE COMPOSITE CYLINDERS: THE POTENTIAL

In section 4 we shall compute the free energy as the work expended for charging the cylinder. This requires knowing the potential at the charged surfaces during this process. If ξ is the linear charge parameter, we need to know the potential for a linear charge $s\xi$ with $0 < s < 1$. We write u instead of $s\xi$.

3.1. Definitions

The polyelectrolyte charges are modeled as one or more continuous cylinders of charge, with a superficial charge density

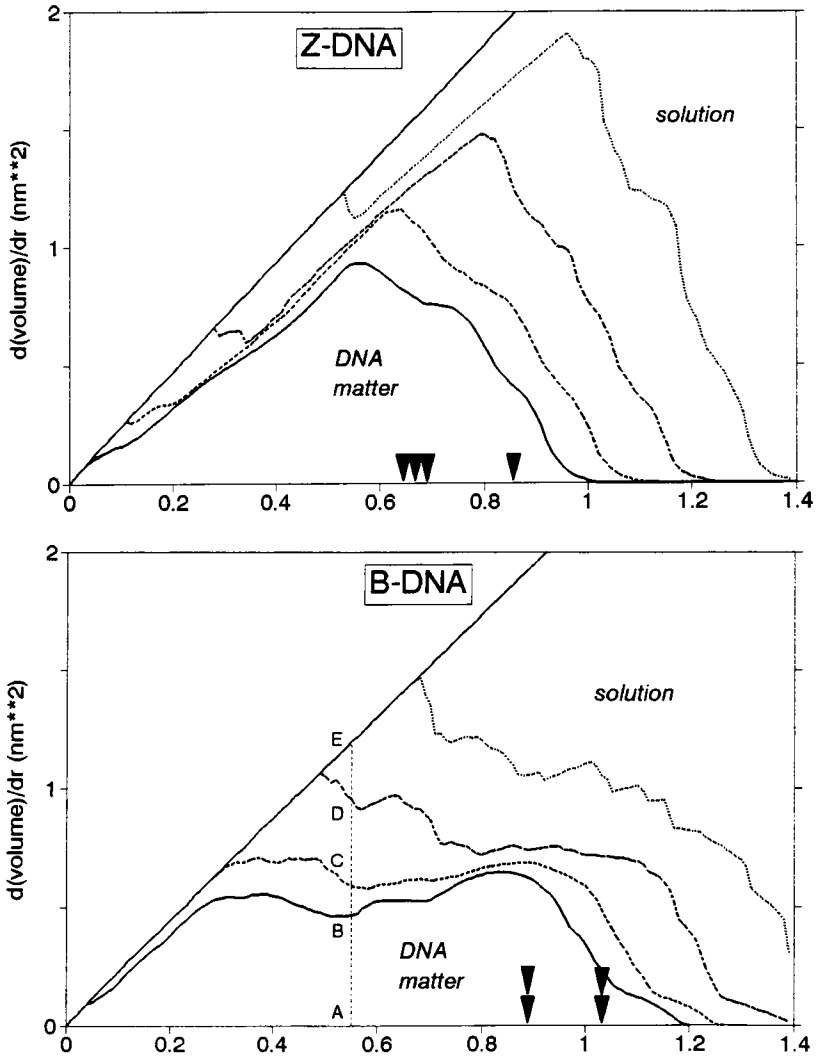

FIGURE 2 Volumes accessible and inaccessible to the center of an ion within a given distance of the DNA axis, represented in a derivative mode. The four curves correspond to the derivative of the volume inaccesible to the center of ions with 0.02, 0.095, 0.235, and 0.4 nm radius, from bottom to top. The straight line corresponds to the derivative of the total cylinder volume. For instance, the volume of DNA within the radius R corresponding to the label A is equal to the area limited by the horizontal axis up to A, the vertical line AB, and the full curve connecting the origin O to B. More precisely, this is the volume inaccessible to an ion of radius 0.02 nm. The volume of solution corresponds to the area limited by the full curve OB and the straight lines BE and EO. The total volume, $\pi R^2 h$, is represented by the area of the triangle OAE. The radial positions of the charged oxygens (r_1 to r_4 in Table 1) are marked by arrows. Top, Z-DNA; bottom, B-DNA.

σ. The *linear charge parameter* ξ is defined by the charge ξe of a cylinder of height l_B, where l_B is the Bjerrum length in water:

$$l_B = e^2/(4\pi\epsilon_0 D_w kT) = 0.72 \text{ nm}, \qquad \text{at } T = 293 \text{ K} \tag{2}$$

where e is the (negative) elementary charge. The linear charge parameter relative to a cylinder of charge at radius b is given by

$$\xi = 2\pi l_B b\sigma/e. \tag{3}$$

The Debye length, λ, is given by

$$\lambda^{-2} = \sum 4\pi l_B (D_w/D(r)) n_i z_i^2. \tag{4}$$

In water and at the molar salt concentration c_m (which corresponds to a number n of each ion per unit volume), one has

$$\lambda^{-2}\,(\text{nm}) = 10.8\, c_m z^2. \tag{5}$$

We now restrict the analysis to the case of a salt in which the anion and cation have the same valency z (a positive number). We designate by ϕ the reduced potential, that is, the potential times e/kT, where e is the electronic charge. With this convention ϕ is positive for a polyanion. In the cylindrical geometry, the Poisson-Boltzmann equations are

$$(1/r)\, d(rD(r)\, d\phi/dr)/dr = D(r)(\lambda^2 z)^{-1} \sinh(z\phi) \tag{6}$$

$$(d\phi/dr)_b = -4\pi l_B (D_w/D(r))\sigma/e = -2(D_w/D(r))\xi/b \tag{7}$$

In Eq. 6, the right side is the charge concentration divided by $\epsilon_0 kT$. The central expression in Eq. 7 is the electric field discontinuity on crossing a charged surface with surface charge density σ. (The presence of the dielectric constant of water in Eqs. 4 and 7 results from the definition of l_B, Eq. 2. The product $l_B D_w$ is in fact independent of D_w. And the product $\lambda^{-2} D(r)$ is independent of $D(r)$.)

It is convenient to introduce the scaling length l_e for the variation of the electric field (5):

$$l_e = (d\phi/dx)/(d^2\phi/dx^2). \tag{8}$$

At the surface of a charged plane, the scaling length l_e^P is given by

$$(1/l_e^P)^2 = (1/\lambda)^2 + (1/Th)^2, \tag{9}$$

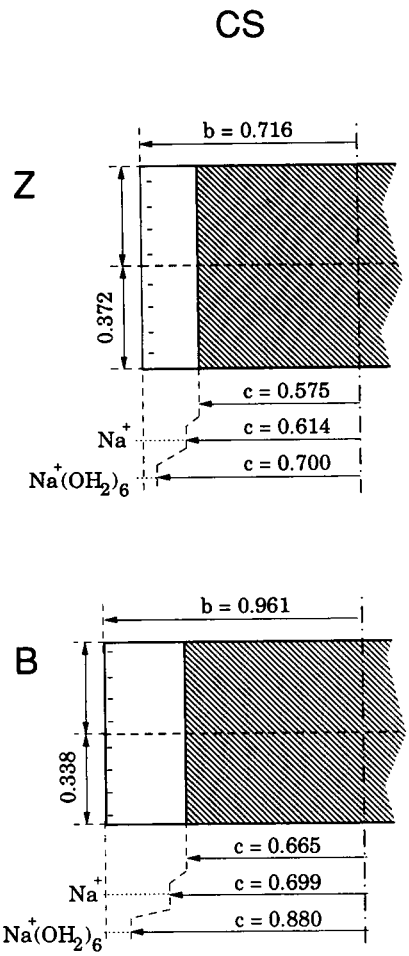

FIGURE 3 CS model of DNA (cylinder with sheath). The model includes a core inaccessible to the center of ions and a sheath accessible to the center of ions, within the charge radius. The radius of the core varies according to the ionic radius. For each ionic radius, the volume of the sheath is larger for B-DNA than for Z-DNA.

where the (positive) thickness Th is

$$Th = (2\pi l_B z\sigma/e)^{-1}. \quad (10)$$

The linear (Debye-Hückel) and nonlinear regimes correspond to $Th > \lambda$ and $Th < \lambda$, respectively.

- The ionic charge concentration at the surface is equal to $-\sigma/l_e^P$.
- A thickness l_e^P next to the surface of the plane includes a counter-ionic charge equal to $\sigma(e-1)/e$ and $\sigma/2$ in the linear and nonlinear limits, respectively.

These results are approximately valid for a strongly charged cylinder ($\xi > 0.5$) with the same surface charge density s when the salt concentration is not too low. In the following sections, we shall make use of an algebraic approximation to the surface potential of a simple cylinder with radius b, $\phi(\xi, b)$, Eqs. A3–A6, based on earlier studies of the surface potential, which are summarized in Appendix A.

3.2. The cylinder with core and sheath

Let u be the linear charge parameter of the charged cylinder surface (radius b) and u_{sh} that of the ions contained in the sheath; note that $u > 0$ and $u_{sh} < 0$ for a polyanion. We observe that starting at radius b_+, immediately beyond radius b, the potential, field, and ionic distribution are the same as if the entire charge $u' = u + u_{sh}$ were at the surface. In particular, the potential ϕ_{CS} at radius b is equal to that of a simple cylinder with linear charge parameter u'. Hence

$$\phi_{CS}(u,b_+) = \phi(u',b) \quad (11)$$

where ϕ is given by Eqs. A3–A6. For evaluating $\phi_{CS}(u,b)$ by Eq. 11, one must know u', or again u_{sh}, the charge in the sheath, which is in itself an interesting quantity. We therefore derived an approximate formula for u_{sh} (Appendix B, Eq. B8). However, the error in this formula reaches 20%, and this is too large for the present problem. We therefore use a different procedure, in which the surface potential $\phi_{CS}(u,b_+)$ and the net charge u' are computed together, iteratively. This procedure will also apply to the cylinder with porous sheath, which is considered in the next section.

The procedure is based on the integration of the Poisson-Boltzmann equation, starting from the surface of the core ($r = c$) and up to the outer radius b. The surface of the core being uncharged, the electric field at c is zero. We guess the value of the potential at c and propagate it by a fourth-order Runge-Kutta procedure up to $r = b$. The potential is continuous across b, but the field is discontinuous, with a jump of $-2u/b$. We thus obtain trial values of the potential and electric field at $r = b_+$. These could be propagated on to infinity, where they should become zero; if they did not, one would repeat the computation with another starting value of the potential at $r = c$, until the process converges. This is the usual numerical procedure for solving the Poisson-Boltzmann equations. It is rather slow, and care is required to ensure convergence, particularly in very low salt. Instead, we shall use our knowledge of the field and potential of a simple cylinder of radius b, as follows. We use the trial value of the electric field at b_+ to compute the linear parameter u' of the total charge within radius b_+ by Eq. 7:

$$u' = -(b/2)\, d\phi_{CS}(u,b_+)/dr. \quad (12)$$

At b_+ and beyond, only solution is present. Therefore the potential $\phi_{CS}(u,b_+)$ should be equal to the potential of the simple cylinder $\phi(u',b)$, as stated in Eq. 11. If it is in fact larger (or smaller) than $\phi(u',b)$, the computation is repeated with a smaller (or larger) initial potential $\phi_{CS}(u,c)$, until convergence is obtained.

In this way we obtain the potential, the field, and the linear charge parameter u' at the charged surface. From the latter we derive the charge parameter for the sheath u_{sh}, which is equal to $u' - u$. The plots of $-u_{sh}$ versus u (Fig. 4) show that the inner screening is quite significant and that it is larger for B-DNA than for Z-DNA, as expected. The potential will be used later to compute the free energy.

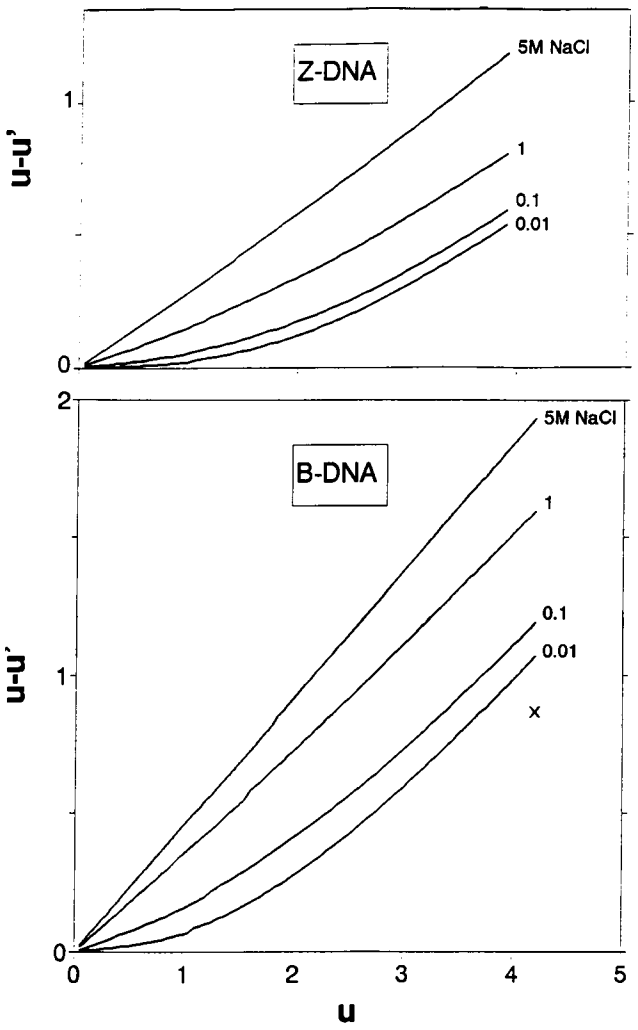

FIGURE 4 The ionic charge in the sheath as a function of the polyelectrolyte charge for the CS models of B- and Z-DNA, at various salt concentrations and for a 0.095-nm ionic radius. The charge in the sheath is much larger in the case of B-DNA. The charges are represented by the corresponding linear charge parameter (u_{sh}, u). The cross is the charge in the grooves computed for an atomic B-DNA structure, using pointlike ions and no added salt (see the Discussion section).

3.3. The cylinder with core and porous sheath

As in section 3.2, the potential is obtained by integration of the Poisson-Boltzmann equations. Starting either from the axis or from a radius so small that the ions within it can be neglected, the integration takes place in the porous medium, across the two charged surfaces and up to the radius a, beyond which only solution remains. In the porous medium, the Poisson-Boltzmann is still given by Eq. 6, with the appropriate values of the dielectric constant and of the Debye length l, namely, their weighted average over the three components of the porous medium. The dielectric constant, which appears on the left side of Eq. 6, is thus given by Eq. 1. On the right side, the product $D(r)\lambda^{-2}$ is proportional to the ionic concentrations in zero potential (n_i), as shown by Eq. 4 for the case of a fluid. In the case of the porous medium, where a fraction $(1 - f_{DNA}(r) - f_{forb}(r))$ of the volume is inaccessible to ion centers, the weighted average of the ionic concentration is reduced in the same proportion. So is λ^{-2}, the expression of which becomes therefore

$$\lambda^{-2} = \sum 4\pi l_B (D_w/D(r))\, n_i (1 - f_{DNA}(r) - f_{forb}(r)) z_i^2 \quad (13)$$

instead of Eq. 4. The Poisson-Boltzmann equation (Eq. 6) is otherwise unchanged. The electric field discontinuity across a charged surface is still given by Eq. 7. The discontinuities of the field at the charged surfaces are

- for B-DNA,

$$-(1/2) * 2u(D_w/D(r_1))/r_1, \qquad \text{located at } r_1,$$

and

$$-(1/2) * 2u(D_w/D(r_2))/r_2, \qquad \text{located at } r^2;$$

- for Z-DNA,

$$-(3/4) * 2u(D_w/D(b'))/b' \qquad \text{at } b',$$

and

$$-(1/4) * 2\,u(D_w/D(r_4))/r_4 \qquad \text{at } r_4,$$

where b' is the average of r_1, r_2, and r_3. The variation of the dielectric constant is continuous and therefore creates no discontinuity in the field.

By integration one obtains values for the potential ϕ_{CPS} and the field at $r = a$. The total charge within radius a is

$$u' = -(a/2)\, d\phi_{CPS}(u,a)/dr. \quad (14)$$

The value of the potential $\phi_{CPS}(u,a)$ is compared to $\phi(u',a)$, and the procedure is iterated, as in section 3.2.

3.4. The electrostatic free energy

The electrostatic free energy F_{el} per unit charge (i.e., per phosphate) is the work performed upon charging the composite cylinder (Fixman, 1982). For Z-DNA and B-DNA in the CS model:

$$F_{el,CS} = kT \int_0^1 \phi_{CS}(s\xi,b)\, ds, \quad (15)$$

where $\phi_{CS}(s\xi,b)$ is the relevant reduced potential ($\phi^z{}_{CS}$ or $\phi^B{}_{CS}$) at radius b during the charging process, that is, when the linear charge parameter is $u = s\xi$.

For B-DNA in the CPS model:

$$F^B_{el,CPS} = kT \int_0^1 \phi_{CPS}(s\xi, r_1) \times (1/2)\, ds + \phi_{CPS}(s\xi, r_2) \times (1/2) ds. \quad (16)$$

For Z-DNA in the CPS model:

$$F^Z_{el,CPS} = kT \int_0^1 \phi_{CPS}(s\xi, b') \times (3/4)\, ds + \phi_{CPS}(s\xi, r_4) \times (1/4) ds. \quad (17)$$

3.5. Propagation of errors

The free energies F^Z_{el} and F^B_{el} (Eqs. 15–17) and their difference are affected by errors in the surface potential ϕ_{CS} or ϕ_{CPS} of the composite cylinder. One source of error of these potentials lies in the surface potential ϕ of the simple cylinder (Eqs. A3–A6), the error of which reaches 5%, as stated in Appendix A. However, for most values of u, the error is much less. Furthermore, the errors compensate rather than accumulate when one takes the difference of the free energies. Therefore, the resulting relative error, even on the FED, is expected to be small. We have tested this in the CPS model, for an ionic radius of 0.095 nm, and for salt concentrations ranging from 0.1 to 4 M. In this range, the maximum error on the free energy was 2.5%, and 4% on the FED.

4. RESULTS

4.1. The electrostatic free energy

The electrostatic free energies and their difference are represented in Figs. 5 and 6 for the CS and CPS models, respectively, for different ionic radii. The results are similar for the two models, and they resemble that of the planar model (Guéron and Demaret, 1992b), even though the three representations of DNA are rather different. This indicates that the results are not dependent on artifactural details of the

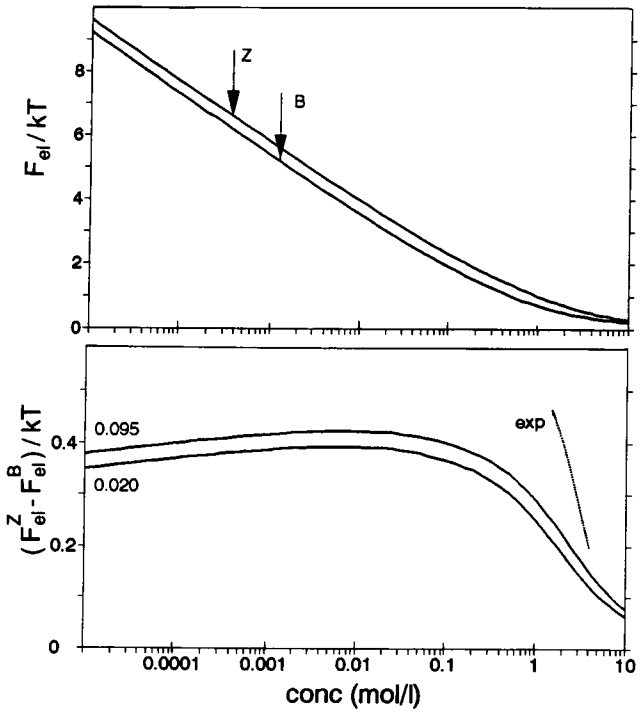

FIGURE 5 (*a*) Electrostatic free energy per phosphate of B-DNA and Z-DNA in the CS model for two ionic radii, 0.095 and 0.4 nm. (*b*) *Electrostatic* FED per phosphate as a function of monovalent salt concentration for 0.02 and 0.095 nm ionic radii. The dotted line corresponds to the *total* FED derived from experiment (Pohl, 1983). It is shifted upward by 0.34 kT units for clarity. In the comparison with theory, it is only the *slope* versus salt concentration, not the absolute value of the FED, which is significant.

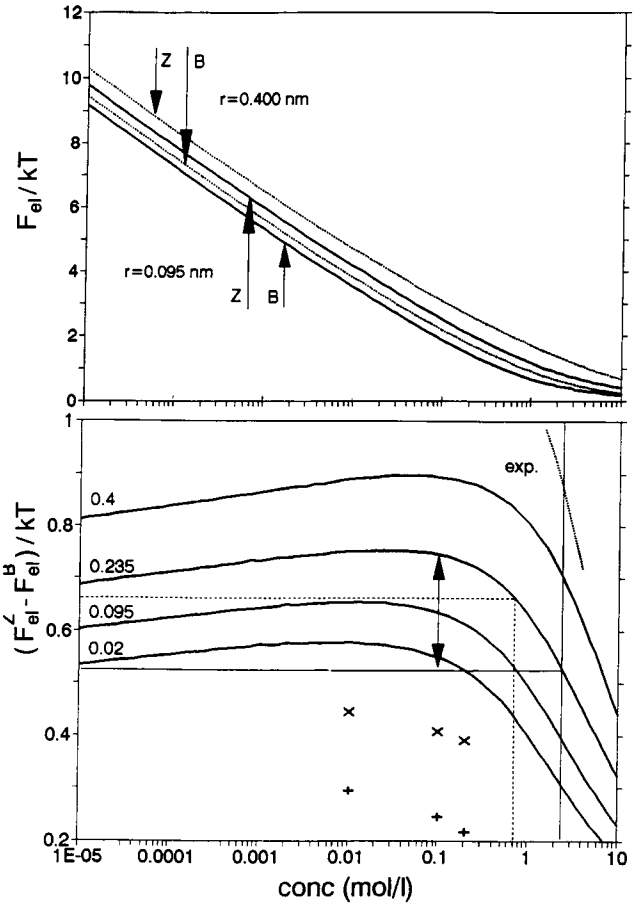

FIGURE 6 (*a*) Electrostatic free energy per phosphate of B-DNA and Z-DNA in the CPS model for two ionic radii, 0.095 and 0.4 nm. (*b*) *Electrostatic* FED per phosphate as a function of monovalent salt concentration for ionic radii of 0.02, 0.095, 0.235, and 0.4 nm. As in Fig. 5 *b*, the dotted line is derived from experiment (Pohl, 1983), and only the slope versus salt concentration is significant. The vertical line at 2.4 M corresponds to the observed B-Z transition of poly d(CG). Assuming an ionic radius of 0.235 nm (see text), the nonelectrostatic FED, indicated by the full horizontal, is therefore $-0.53kT$. Similarly, the dashed lines correspond to the B-Z transition of poly d(mCG), which is observed at 0.7 M NaCl (Behe and Felsenfeld, 1981). The crosses are the results, up-shifted by 0.6, of a study using atomic structures for alternating CG (x) and 5-methyl-CG (+) (see Discussion).

representation and justifies the earlier use of the planar model for explaining the B-Z transition. Further support for the robustness of the model is provided by the modest effect produced by a variation of its parameters. We tested the effect of placing all phosphates at the average radius b instead of using the distribution expressed by Eqs. 16 and 17, for an ionic radius of 0.095 nm, in the CPS model. The FED increases by 7% in 1 M salt, increasing progressively up to 13% in 10^{-5} M salt, with little effect on the high-salt slope. Another test consists in changing the radial distances of phosphates by +10% and −10%. This shifts the FED by $-0.08\ kT$ and by $+0.09\ kT$, respectively, independently of the salt concentration.

Starting from very low salt concentrations, the electrostatic FED increases slowly, favoring the B form, up to ~0.1–1 M. At higher concentrations the difference decreases

strongly, driving the B-Z transition. The strong decrease begins at salt concentrations for which the Debye length is small enough to influence the scaling length (Eq. 8). *This corresponds to the transition from the nonlinear to the linear electrostatic regime, which may therefore be a factor in the high-salt B-Z transition.*

The electrostatic free energy increases with the ionic radius, nearly independently of the salt concentration. This is due mainly to the field energy in the region forbidden to the center of the ion, surrounding the polyelectrolyte (Guéron and Demaret, 1992a).

4.2. Direct comparison with experiment: the slope in high salt

For concentrations between 1.5 and 5 M, Pohl (1983) could derive the total FED from a study of the B-Z transition in d(CG) oligomers of different lengths. His results correspond to the dotted curve in Figs. 5 and 6 (vertically shifted for clarity; the *total* FED is zero at 2.4 M NaCl). It displays two main features. First, between 2 and 5 M salt, there is a linear dependence of the FED on the logarithm of the salt concentration. The slope corresponds to an increment of 0.21 in kT units per mole of phosphate when the salt concentration is doubled. We shall denote this value as $\delta^E(2, 4)$ or simply δ^E, where E stands for experimental, and we shall use it for the comparison between theory and experiment. The second feature is a reduction in the slope for salt concentrations between 2 and 1.5 M.

The theoretical slopes $\delta^T(2, 4)$ and the curvature in lower salt are in qualitative agreement with the experimental result. The slope of the planar model (Guéron and Demaret, 1992b) is equal to the experimental one, whereas those of CS and CPS models are lower by a factor of 2 to 3, depending on the model and the ionic radius (Table 2).

In the planar model, B-DNA is overscreened, Z-DNA is not screened, and one obtains the largest theoretical slope. In the CS model, there is too much screening for the Z form because all the phosphate charges are lumped at the average radius b, so that too much solution is included within the radius of charge.

Let us compare the plain and rather successful CS model with the simple cylinder. In the CS model, the charges are placed close to the true radial distance of the DNA charges, and they are bathed by solution on both sides. For a 0.02-nm ionic radius, the FED slope is $0.29\delta^E$ (Fig. 5). To show the contribution of the sheath to this result, we increase c, the core radius, up to b, thus eliminating the sheath, all other dimensions being unchanged. The slope is reduced to $0.14\delta^E$ (not shown).

In the simple cylinder, the radius of the cylinder is approximately that of DNA, 1 nm for B-DNA, and 0.9 nm for Z-DNA. This model gives an FED slope of only $0.013\delta^E$ (Frank-Kamenetskii et al., 1985; Lukashin et al., 1991). Since the cylinder is impenetrable, the potential outside is independent of the radius chosen for the charge distribution. Traditionally, the charges are located at the surface. In this case, the source of the difference from the CS model with zero-size sheath is that the charges are placed at an incorrect and larger radius. Alternatively, we could place the charges of the simple cylinder at the correct radius, the same as in the CS model. The (erroneous) smallness of the FED slope of the simple cylinder is then ascribed to the insulating layer between the charges and the solution.

The CPS model is the most careful with regard to the distribution of DNA matter and charge and to the treatment of the dielectric constant. Its FED values should therefore be the most trustworthy. The value of $-\delta^{CPS}$ increases progressively with ionic radius, up to 0.1 kT, or $0.5\delta^E$ for a radius of 0.4 nm (Table 2). It remains approximately constant between 0.4 and 0.6 nm and then decreases (not shown). The slope is less for smaller ions because they provide internal screening even for Z-DNA. In the case of very large ions, the reduction is due to the lack of internal screening even for B-DNA.

In this section we have compared the slope of the FED versus salt concentration in high salt, as derived from theory and from experiment. This is the only direct test of the theory. The primary success of the sheathed-cylinder models is the prediction of a slope that is in the range of the experimental one, δ^E. We take this as a strong indication of the validity of the models, and especially of the most detailed one, the porous-sheath cylinder (CPS).

4.3. Indirect comparisons with experiment

Further comparisons can be made if we introduce the experimental value, 2.4 M, of the NaCl concentration for the B-Z transition (Pohl, 1983). At this concentration, the total FED is zero. Therefore, according to Fig. 6, and for an ionic radius of 0.235 nm, the nonelectrostatic FED is $-0.53kT$, or −1.27 kJ/mol phosphate.

TABLE 2 Experimental and theoretical slopes δ*

	Experimental‡	CS	← CPS →			
Ion radius	—	0.095	0.02	0.095	0.235	0.4
δ§	−0.210	−0.072	−0.075	−0.085	−0.097	−0.110
δ¶	1	0.34	0.36	0.41	0.46	0.52

*This is the derivative of the electrostatic FED with respect to the natural log of salt concentration, expressed as the FED increment when the concentration is doubled, at a salt concentration of 2.4 M.

‡Derived from Pohl (1983).

§In kT units per phosphate, at 22°C (RT = 2.4 kJ/mol).

¶Relative values.

(*a*) We assume that the nonelectrostatic free energy is independent of ionic strength. Then the total FED at any salt concentration is equal to the electrostatic FED minus 1.27 kJ, and it can be read off Fig. 6 as the distance from the electrostatic difference curve to the full horizontal line. The total FED increases with salt concentration up to a broad maximum of 0.55 kJ/mol phosphate at 0.04 M salt. A similar trend is observed in supercoiled DNA (Peck and Wang, 1983; Singleton et al., 1982); however, the total FED increases more strongly with salt, the maximum is higher (1.36 kJ/mol phosphate), and it is reached at 0.2 M NaCl. In the comparison, one should keep in mind that the experiments are carried out on supercoiled DNA and in 90 mM Tris-borate buffer and that the derivation of the total FED involves a statistical mechanics model and a best-fit procedure.

(*b*) With 5-methylcytosine (the $d(mCG)_n$ sequence), the B-Z transition takes place at 0.7 M NaCl (Behe and Felsenfeld, 1981), as marked by the dashed lines in Fig. 6. If we neglect the modest changes in shape between the methylated and nonmethylated sequences, the theoretical electrostatic FED is not affected. The change in nonelectrostatic FED has been ascribed to the hydrophobicity of the methyl group (Fujii et al., 1982). Using the dashed horizontal line, we see that the total FED in 0.1 M NaCl is smaller (in the ratio of 0.4 to 1) than for the nonmethylated compound, again in qualitative agreement with observations (a ratio of 0.34 to 1) in Tris-borate buffer (Zacharias et al., 1988).

The existence of a maximum in the FED is also in line with experiment. Furthermore, the theoretical FED in very low salt (10^{-5} M) is quite small, suggesting the possibility of a transition to the Z-form in low salt. The low-salt properties of the (CG) and (mCG) duplexes will be discussed elsewhere (Guéron and Demaret, in preparation).

(*c*) How is the high-salt transition affected by the size of the counter-ion? Assuming that the nonelectrostatic FED is independent of the counter-ion, the B-Z transition should occur at the ionic concentration determined by the intersection of the appropriate curve in Fig. 6 with the horizontal line (e.g., 0.75 M for an ionic radius of 0.095 nm). For ionic radii close to 0.235 nm, we find that the transition concentration c_t varies as

$$\log (c_t/2.4) \approx 7(r - 0.235). \quad (18)$$

From sodium to rubidium, the bare ion radius increases by 0.053 nm, so the transition concentration with rubidium counter-ions should be 1.1 M more than with sodium, whereas the experimental increment is 0.4 M (Soumpasis et al., 1987a). The discrepancy may be due to the value of the ionic radius, which depends on the extent of ionic hydration, and this can differ according to the radius of the naked ion.

5. DISCUSSION

5.1. This model

The model presented here includes cylindrical representations of nucleic acids and the computation of their electrostatic free energy in the Poisson-Boltzmann theory. The results were described in the previous section. The qualitative agreement with a variety of experimental results supports the premises of the theory: that the main feature of the electrostatics of the B-Z transition is the immersion of B-DNA phosphates in the solution and that this feature can be described by a cylindrical model in the Poisson-Boltzmann framework.

These premises find further support in the resemblance of the results obtained in the different models (the CS and CPS cylinders and the planar model) and in the difference between these results and those of the simple cylinder models, the phosphates of which, if placed at the proper radius, are insulated from the solution.

The success of the composite cylinder models suggests that the features which they do not describe in detail have a modest influence on the electrostatics of the B-Z transition. But they might be involved in the quantitative discrepancies with experiment (e.g., of the high-salt slope δ).

DNA structure

The effect of cylindrical averaging may be studied by comparing our results with those of Poisson-Boltzmann studies that use the atomic DNA structure. In Fig. 4, we show (X) the charge in the grooves of B-DNA, without added salt, as computed in one such study (Pack et al., 1991). The result compares well with the charge in the sheath of the CS model. In Fig. 6 we show (X, +) the salt-dependent part of the free energy, for NaCl concentrations of 0.01, 0.1, and 0.2 M from another study (Pack et al., 1986, 1991). Their variation with salt is similar to ours. In another study using the atomic geometry, the high-salt slope is one-half of the experimental one (B. Honig, private communication); again, this result is quite similar to ours.

Structure and binding of ions

There is experimental and theoretical evidence for the dehydration of cations interacting with phosphates or other groups (as mentioned in section 2.3). The description of ions by a single radius, which could be valid only if the hydration is invariant, is therefore an arguable simplification.

This question is related to that of ion binding. In view of the high local concentrations of cations in the vicinity of the polyelectrolyte, binding sites with a dissociation constant as large as 1 M will be partly occupied, and this will affect the ionic distribution and the free energy. Ion binding has been incorporated into polyelectrolyte theory (Guéron and Weissbuch, 1981; Delville, 1984). The nature, number, and affinity of binding sites must be provided independently. A theoretical analysis (Matthew and Richards, 1984) assigns more bound ions to Z- than to B-DNA.

Polyelectrolyte theory

We have referred above to general arguments suggesting that the neglect of ion-ion correlations by the Poisson-Boltzmann theory is less serious for properties of polyelectrolytes in

solution than for properties of ionic solutions (Fixman, 1979). Comparative studies of DNA by Poisson-Boltzmann theory and by a Monte Carlo approach support this view (Klein and Pack, 1983; Pack et al., 1991).

5.2. A treatment of inter-ion correlations

There is another model that predicts a slope of the B-Z transition comparable to the experimental one (Soumpasis, 1984). In contrast to the present model, which emphasizes the geometrical differences between B-DNA and Z-DNA, the earlier model gives much attention to inter-ion correlations. In view of the high salt concentration at the B-Z transition of poly d(CG), it therefore avoids the mean-field Poisson-Boltzmann theory and treats the interactions between ions (including phosphates) with an approach based on the potential of mean force. The ions are hard spheres, with a unique closest approach parameter σ, denoted here as σ_s. The computation of the free energy involves approximations and is carried out to leading order. One finds that the slope δ is strongly dependent on σ_s. Agreement with the experimental slope in high salt is obtained for $\sigma_s = 0.49$ nm. Agreement of the theoretical salt concentration of the transition with the experimental one is dependent on the assumption that the nonelectrostatic FED is zero. There is no reduction of the FED in low salt, in contrast to the experimental results (Singleton et al., 1982; Peck and Wang, 1983).

The theory has also been used for the computation of the transition concentration in solutions of different monovalent cations (Soumpasis et al., 1987a). By adjusting σ_s as before, one obtains agreement with experimental data for Na, K, Rb, and Cs. Other ions, such as lithium, ammonium, and ammonium derivatives, are considered to be in a different category.

A problem with this approach is that the complexity of the potential of mean force computations leads to the use of simplified models, which may be ill-adapted to the treatment of the correlations that the theory is meant to account for. A severe simplification is in the description of DNA: the effect of solute ions on the electrostatic interaction between phosphates, which governs the electrostatic free energy, is computed as if *all of the neutral DNA matter* (*i.e., bases and sugars*) were absent and replaced by the solution (Soumpasis, 1984; Soumpasis et al., 1987b; Soumpasis and Jovin, 1987; Garcia and Soumpasis, 1989; Klement et al., 1990). This is a poor description of DNA and its interface with the solution, and it must bring more solute ions close to phosphates than there should be on the average. A more recent model does take neutral DNA in account, but its application to the B-Z transition has not been reported (Klement et al., 1991).

There is also a problem with the computation of the transition concentration. The assumption that the nonelectrostatic FED is zero lacks theoretical justification. In the Poisson-Boltzmann model (this work), the nonelectrostatic FED (equal and opposite to the electrostatic FED at the transition concentration of 2.4 M) is large; setting it to zero would lead to a transition concentration very much higher than that observed (Fig. 6).

6. CONCLUSION

In the present work we have developed the notion that the principal feature contributing to the electrostatic FED between B-DNA and Z-DNA is the larger volume available for screening of the phosphate charges in the grooves of B-DNA. Cylindrical models incorporating this feature were described, and their electrostatic free energy was computed in the Poisson-Boltzmann theory. Our results are in qualitative agreement with experimental data, which may be interpreted directly or indirectly in terms of the electrostatic free energy.

The simplicity of the model entails a risk of simplification or even distortion. But it has several advantages. The concepts, for instance the characteristic length l_e of the electric field at the surface of a polyelectrolyte, or the charge in the sheath u_{sh}, or the cylindric averaging of DNA matter, are easily understood. The smallness of the computational load makes it easy to vary either the properties of the model, such as the averaging of the DNA charges or the structure of the sheath representating the DNA grooves, or the parameters of the problem, such as ionic concentration and ionic size. This has helped us to determine and emphasize the features that appear to be most significant for the electrostatics of the B-Z transition.

We thank J. Lepage for help in the drawing of Fig. 1. This work was begun while J-P. Demaret was at the Laboratoire de Biochimie de l'Ecole Polytechnique.

APPENDIX A: THE SURFACE POTENTIAL OF A PLANE AND OF A SIMPLE CYLINDER

We again consider the case when salt anion and cation have the same valence. The surface potential ω of a plane is given by (Weisbuch and Guéron, 1981)

$$\omega = (2/z) \log (x + (x^2 + 1)^{1/2}) \equiv (2/z) \sinh^{-1} x \qquad \text{(A1)}$$

with

$$x = \lambda/Th \qquad \text{(A2)}$$

where λ and Th are defined by Eqs. 4 and 10, respectively.

A simple cylinder is one with neither sheath nor outer matter. Precise algebraic approximations have been derived (Stigter, 1975; Weisbuch and Guéron, 1981) for its reduced surface potential $\phi(\xi, b)$. For a highly charged cylinder ($1 < \xi$) we started from the planar potential and computed appropriate corrections:

$$\phi(\xi, b) = \omega + \phi_{corr} \qquad \text{(A3)}$$

where ω is the surface potential of a plane having the same surface density σ (Eq. 14)and

$$\phi_{corr} = -(2/z)/[z\xi - 0.45 + 1.8/x^{1/2} + 3\epsilon/x]. \qquad \text{(A4)}$$

In this expression, ϵ is the ratio of the cylinder radius b to the Debye length λ. Using Eq. 3, we have

$$x \equiv \lambda/Th = z\xi/\epsilon. \qquad \text{(A5)}$$

In the case of a weakly charged cylinder ($\xi < 1$), we found that the deviation of the surface potential from Debye-Hückel (Stigter, 1975) is well represented by the factor

$$1/(1 + \xi^2/(5 + 20\epsilon^2)).$$

Hence

$$\phi(\xi, b) = 2\xi[\log(1 + 1/\epsilon)]/(1 + \xi^2/(5 + 20\epsilon^2)). \quad \text{(A6)}$$

The surface potentials given by Eqs. A3 to A6 have been computed to be between $\xi = 0$ and $\xi = 5$, a range that includes the values used in the computation of the free energy, and for ϵ between 10^{-2} and 10, which for DNA corresponds to monovalent salt concentrations between 10^{-5} and 10 mol/liter. In this entire range, the algebraic expression for the surface potential deviates by less than 5% from the value obtained by numerical integration of the Poisson-Boltzmann equation with a fourth-order Runge-Kutta algorithm. The largest errors occur near $\xi = 1$, which is as expected, since this is the connection point between the small and large ξ cases, ϕ_{corr} being correct in the two limits of $\xi \to 0$ and $\xi \to \infty$.

APPENDIX B: ESTIMATION OF THE CHARGE OF THE CYLINDER WITH SHEATH (CS MODEL)

This estimation is based on the scaling length of the electric field, the derivation of which for a cylinder is similar to that used previously for the plane (Guéron and Weisbuch, 1980). We start from the Poisson-Boltzmann equations. In water, we obtain from Eqs. 6 and 7:

$$d^2\phi/dr^2 + (1/r)\, d\phi/dr = (\lambda^2 z)^{-1} \sinh(z\phi) \quad \text{(B1)}$$

$$(d\phi/dr)_b = -2\xi/b. \quad \text{(B2)}$$

The equations for a plane with the same surface charge density σ would be the same except for the absence of the $(1/r)(d\phi/dr)$ term. We take the ratio of the equations at $r = b$:

$$(1/l_e - 1/b) = \epsilon^2 \sinh(z\,\phi(\xi, b))/(2\xi z\, b). \quad \text{(B3)}$$

This gives the scaling length at the surface of the cylinder as a function of the potential. It is always smaller than b. Introducing the counter-ionic charge concentration ρ:

$$\rho(b)/e = -2nz \sinh(z\phi(\xi, b)) = -\sinh(z\,\phi(\xi, b))/(4\pi l_B z\lambda^2) \quad \text{(B4)}$$

we have

$$(1/l_e - 1/b) = -2\pi b l_B(\rho(b)/e)/\xi. \quad \text{(B5)}$$

Comparing to the plane with the same surface charge density, one also has

$$(1/l_e - 1/b)l_e^P = \sinh(z\phi(\xi, b))/\sinh(z\omega). \quad \text{(B6)}$$

Next, we estimate the linear charge parameter corresponding to the ions in the sheath (u_{sh}) in two limiting cases, $(b - c) << l'_e \leq b$ and $l'_e << (b - c) \leq b$, where l'_e, the scaling length for the electric field at b_+, is given by Eq. B3, in which ξ is replaced by u'. The general case is then treated by interpolation.

In the first case, the ionic concentration is roughly constant in the sheath. Hence, to first order in $(b - c)/b$,

$$u_{sh}^{(1)} = -2\pi b(b - c)l_B\rho(b)/e = -u'(b - c)((1/l'_e) - (1/b)). \quad \text{(B7)}$$

In the second case, screening takes place over a length much smaller than $(b - c)$, so that the screening ions are symmetrically distributed around the charged surface. Hence $u_{sh}^{(2)} = -u'$.

A simple interpolation between the two cases is

$$u_{sh} = -u'(1/l'_e - 1/b)/(1/(b - c) + 1/l'_e - 1/b). \quad \text{(B8)}$$

The potential at the charged surface for a given u' is obtained by Eqs. A3–A6 and B3, in which u' is substituted for ξ and l'_e for l_e. Eq. B8 provides the relation between u_{sh} and u', and hence between u' and u. Last, the surface potential is obtained by Eq. 11.

This procedure was checked against values of u_{sh} derived from the surface potential computed by integration of the Poisson-Boltzmann equation (Fig. 4). The results are fairly good within the range of $\xi = 0$ to 5 and for salt concentrations between 10^{-2} and 10 M. The maximum relative error on u_{sh}, reached in the case of 1 M salt, is 20%.

REFERENCES

Arnott, S., P. J. Campbell-Smith, and R. Chandrasekaran. 1975. Atomic coordinates and molecular conformation for DNA-DNA, RNA-RNA and DNA-RNA helices. *In* CRC Handbook of Biochemistry and Molecular Biology. Vol. 2. G. D. Fasman, editor. CRC Press, Cleveland. 411–423.

Behe, M., and G. Felsenfeld. 1981. Effects of methylation on a synthetic polynucleotide: the B-Z transition in poly(dG-m^{5}dC)·poly(dG-m^{5}dC). *Proc. Natl. Acad. Sci. USA.* 78:1619–1623.

Behe, M., G. Felsenfeld, S. Chen Szu, and E. Charney. 1985. Temperature-dependent conformational transitions in poly(dG-dC) and poly(dG-m^{5}dC). *Biopolymers.* 24:289–300.

Connolly, M. L. 1983. Analytical molecular surface calculation. *J. Appl. Cryst.* 16:548–558.

Delville, A. 1984. Interactions between ions and polyelectrolytes. A note on determination of ionic activities, with reference to a modified Poisson-Boltzmann treatment. *Biophys. Chem.* 19:183–189.

Fixman, M. 1979. The Poisson-Boltzmann equation and its application to polyelectrolytes. *J. Chem. Phys.* 70:4995–5005.

Fixman, M. 1982. The flexibility of polyelectrolyte molecules. *J. Chem. Phys.* 76:6346–6353.

Frank-Kamenetskii, M. D., A. V. Lukashin, and V. V. Anshelevich. 1985. Application of polyelectrolyte theory to the study of the B-Z transition in DNA. *J. Biomol. Struct. Dyn.* 3:35–42.

Fujii, S., A. H. J. Wang, G. van der Marel, J. H. van Boom, and A. Rich. 1982. Molecular structure of (m^{5}dC-dG)$_3$: the role of the methyl group on 5-methylcytosine in stabilizing Z-DNA. *Nucleic Acids Res.* 10:7879–7892.

Fuoss, M., A. Katchalsky, and S. Lifson. 1951. The potential of an infinite rod-like molecule and the distribution of the counter ions. *Proc. Natl. Acad. Sci. USA.* 37:579–589.

Garcia, A. E., and D. M. Soumpasis. 1989. Harmonic vibrations and thermodynamic stability of a DNA oligomer in monovalent salt solution. *Proc. Natl. Acad. Sci. USA.* 86:3160–3164.

Guéron, M., and J. P. Demaret. 1992a. Polyelectrolyte theory 4. Algebraic expression for the Poisson-Boltzmann free energy of a cylinder. *J. Phys. Chem.* 96:7816–7820.

Guéron, M., and J. P. Demaret. 1992b. A simple explanation of the electrostatics of the B-Z transition of DNA. *Proc. Natl. Acad. Sci. USA.* 89:5740–5743.

Guéron, M., and G. Weisbuch. 1979. Polyelectrolyte theory. II. Activity coefficients in Poisson-Boltzmann and in condensation theory. The polarisability of the counter-ion sheath. *J. Phys. Chem.* 83:1991–1998.

Guéron, M., and G. Weisbuch. 1980. Polyelectrolyte theory. I. counter-ion accumulation, site-binding, and their insensitivity to polyelectrolyte shape in solutions containing finite salt concentrations. *Biopolymers.* 19: 353–382.

Guéron, M., and G. Weisbuch. 1981. Polyelectrolyte theory of charged-ligand binding to nucleic acids. *Biochimie (Paris).* 63:821–825.

Hingerty, B. E., R. H. Ritchie, T. L. Ferrel, and J. E. Turner. 1985. Dielectric effects in biopolymers: the theory of ionic saturation revisited. *Biopolymers.* 24:427–439.

Ivanov, V. I., A. T. Karapetyan, and M. M. Minyat. 1987. *In* Structure and Expression. Vol. 2. DNA and Its Drug Complexes. R. H. Sarma and M. H. Sarma, editors. Adenine Press, Guilderland, NY. 205–216.

Klein, B. J., and G. R. Pack. 1983. Calculations of the spatial distribution of charge density in the environment of DNA. *Biopolymers.* 22:2331–2352.

Klement, R., D. M. Soumpasis, E. V. Kitzing, and T. M. Jovin. 1990. Inclusion of ionic interactions in force field calculations of charged biomolecules—DNA structural transitions. *Biopolymers.* 29:1089–1103.

Klement, R., D. M. Soumpasis, and T. M. Jovin. 1991. Computation of ionic distributions around charged biomolecular structures: results for right-handed and left-handed DNA. *Proc. Natl. Acad. Sci. USA.* 88:4631–4635.

Krzyzaniak, A., P. Salanski, J. Jurczak, and J. Barciszewski. 1991. B-Z DNA reversible conformation changes effected by high pressure. *FEBS Lett.* 279:1–4.

Lafer, E. M., A. Möller, A. Nordheim, B. D. Stollar, and A. Rich. 1981. Antibodies specific for left-handed Z-DNA. *Proc. Natl. Acad. Sci. USA.* 78:3546–3550.

Lafer, E. M., R. Sousa, R. Ali, A. Rich, and B. D. Stollar. 1986. The effect of anti-Z-DNA antibodies on the B-DNA-Z-DNA equilibrium. *J. Biol. Chem.* 261:6438–6443.

Lukashin, A. V., D. B. Beglov, and M. D. Frank-Kamenetskii. 1991. Comparison of different approaches for calculation of polyelectrolyte free energy. *J. Biomol. Struct. Dyn.* 9:517–523.

Matthew J. B., and F. M. Richards. 1984. Differential stabilization of A-, B-, and Z-forms of DNA. *Biopolymers.* 23:2743–2759.

Pack, G. R., C. V. Prasad, J. S. Salafsky, and L. Wong. 1986. Calculations on the effect of methylation on the electrostatic stability of the B- and Z-conformers of DNA. *Biopolymers.* 25:1697–1715.

Pack, G. R., G. Lamm, L. Wong, and D. Clifton. 1991. The structure of the electrolyte environment of DNA. *In* Theoretical Biochemistry and Molecular Biophysics. Vol. 1. D. L. Beveridge and L. Lavery, editors. Adenine Press, Schenectady, NY. 237–246.

Peck, L. J., and J. C. Wang. 1983. Energetics of the B-to-Z transition in DNA. *Proc. Natl. Acad. Sci. USA.* 80:6206–6210.

Pohl, F. M. 1976. Polymorphism of a synthetic DNA in solution. *Nature (Lond.).* 260:365–366.

Pohl, F. M. 1983. Salt-induced transition between two double-helical forms of oligo(dC-dG). *Cold Spring Harbor Symp. Quant. Biol.* 47:113–118.

Pohl, F. M., and T. M. Jovin. 1972. Salt-induced co-operative conformational change of a synthetic DNA: equilibrium and kinetic studies with poly(dG-dC). *J. Mol. Biol.* 67:375–396.

Prasad, C. V., and G. R. Pack. 1984. Theoretical study of phosphate interaction with ammonium (1+) ion, with sodium (1+) ion, and with magnesium (2+) ion in the presence of water. *J. Am. Chem. Soc.* 106:8079–8086.

Rosenberg, J. M., N. C. Seeman, J. J. Park Kim, F. L. Suddath, H. B. Nicholas, and A. Rich. 1973. Double helix at atomic resolution. *Nature (Lond.).* 243:150–154.

Sági, J., A. Szemzö, L. Ötvös, M. Vorlicková, and J. Kypr. 1991. Destabilization of the duplex and the high-salt Z-form of poly(dG-methyl^{5}dC) by substitution of ethyl for the 5-methyl group. *Int. J. Biol. Macromol.* 13:329–336.

Singleton, C. K., J. Klysik, S. M. Stirdivant, and R. D. Wells. 1982. Left-handed Z-DNA is induced by supercoiling in physiological ionic conditions. *Nature (Lond.).* 299:312–316.

Soumpasis, D. M. 1984. Statistical mechanics of the B-Z transition of DNA: contribution of diffuse ionic interactions. *Proc. Natl. Acad. Sci. USA.* 81:5116–5120.

Soumpasis, D. M., and T. M. Jovin. 1987. Energetics of the B-Z DNA transition. *In* Nucleic Acids and Molecular Biology. F. Eckstein and D. M. Lilley, editors. Springer-Verlag, Berlin and Heidelberg. 85–111.

Soumpasis, D. M., M. Robert-Nicoud, and T. M. Jovin. 1987a. B-Z conformational transition in 1:1 electrolytes: dependence upon counter-ion size. *FEBS Lett.* 213:341–344.

Soumpasis, D. M., J. Wiechen, and T. M. Jovin. 1987b. Relative stabilities and transitions of DNA conformations in 1:1 electrolytes: a theoretical study. *J. Biomol. Struct. Dyn.* 4:535–552.

Stigter, D. 1975. The charged colloidal cylinder with a Gouy double layer. *J. Colloid Interface Sci.* 53:296–306.

Stirdivant, S. M., J. Klysik, and R. D. Wells. 1982. Energetic and structural inter-relationship between DNA supercoiling and the right- and left-handed Z helix transitions in recombinant plasmids. *J. Biol. Chem.* 257: 10159–10165.

Tondre, C., and R. Zana. 1972. Apparent molar volume of polyelectrolytes in aqueous solutions. *J. Phys. Chem.* 76:3451–3459.

Tondre, C., and R. Zana. 1975. Comments on letter: "Dilatometric study of monovalent counter-ion association with polymethacrylate" (J. Komiyama, Y. Takeda, M. Ando, and T. Tijima. 1974. *Polymer.* 15:468–470). *Polymer.* 16:228–229.

Van de Sande, J. H., L. P. McIntosh, and T. Jovin. 1982. Manganese (2+) and other transition metals at low concentration induce the right-to-left helical transformation of poly(d(G-C)). *EMBO J.* 1:777–782.

Wang, A. H. J., G. L. Quigley, F. J. Kolpak, J. L. Crawford, J. H. van Boom, G. van der Marel, and A. Rich. 1979. Molecular structure of a left-handed double helical DNA fragment at atomic resolution. *Nature (Lond.).* 282: 680–686.

Wang, A. H. J., G. L. Quigley, F. J. Kolpak, G. van der Marel, J. H. van Boom, and A. Rich. 1981. Left-handed double helical DNA: variations in the backbone conformation. *Science (Washington DC).* 211:171–176.

Weisbuch, G., and M. Guéron. 1981. Polyelectrolyte theory. 3. The surface potential in mixed-salt solutions. *J. Phys. Chem.* 85:517–525.

Weisbuch, G., and M. Guéron. 1983. Une longueur d'échelle pour les interfaces chargées. *J. Physique.* 44:251–256.

Zacharias, W., T. R. O'Connor, and J. E. Larson. 1988. Methylation of cytosine in the 5-position alters the structural and energetic properties of the supercoil-induced Z-helix and of B-Z junctions. *Biochemistry.* 27: 2970–2978.